Acta Crystallographica Section B
**Structural Science**
ISSN 0108-7681

# Superspace description of the modulated structure of the metal-salt-hybrid $Bi_{7-\delta}Ni_2Br_{5-2\delta}$ ($\delta$ = 1/9)

**B. Wahl and M. Ruck***

Inorganic Chemistry, Department of Chemistry and Food Chemistry, Dresden University of Technology, D-01062 Dresden, Germany

Correspondence e-mail: michael.ruck@chemie.tu-dresden.de

Received 29 June 2009
Accepted 27 July 2009

The compound $Bi_{7-\delta}Ni_2Br_{5-2\delta} = (Bi_3Ni)_2[Bi_{1-\delta}Br_4]Br_{1-2\delta}$ ($\delta$ = 1/9) is a sub-bromide of the intermetallic phase $Bi_3Ni$. Its crystal structure contains metallic rods, $^1_\infty[Bi_3Ni]$, which are embedded in a salt-like matrix of bromido-bismuthate(III) and bromide anions. The non-stoichiometry originates from the variation of the number $n$ of *trans* edge-sharing octahedra in the $[Bi_nBr_{4n+2}]^{(n+2)-}$ oligomers ($3 \leq n \leq 5$), as well as from vacancies on the sites of the isolated Br atoms. The simplified structure is described in the orthorhombic space group *Cmcm* with $a$ = 4.0660 (4), $b$ = 23.305 (3), $c$ = 17.130 (2) Å. It shows a statistical distribution of vacancies and orientational disorder of the concatenated octahedra. By choosing the modulation vector $\mathbf{q} = \mathbf{a}^*/9 + \mathbf{b}^*/2$, the additional weak reflections of the diffraction pattern can be indexed. In the [3 + 1]-dimensional superspace group $Pmnm(\alpha\frac{1}{2}0)000$, an ordered structure model is achieved. The modulated crystal structure bears a strong resemblance to the somewhat higher oxidized sub-bromide $Bi_{7-\delta}Ni_2Br_5$ ($\delta$ = 1/9).

## 1. Introduction

There is huge interest in compounds with highly anisotropic electrical conductivity, especially in one-dimensional metals (Giamarchi, 2004). One way to obtain such compounds has been pursued in the systems Bi—Ni—*X* *via* partial oxidation of the intermetallic phase $Bi_3Ni$ by halogens *X*. The crystal structure of the intermetallic compound had been described as a distorted hexagonal packing of $^1_\infty[Bi_3Ni]$ rods (Glagoleva & Zhdanov, 1954; Fjellvåg & Furuseth, 1987; Ruck & Söhnel, 2006). In the subhalides, the $^1_\infty[Bi_3Ni]$ rods are retained unchanged, but their connectivity is reduced. The insertion of non-conducting parts, like halogenide ions in $Bi_{12}Ni_4I_3$ (Ruck, 1997) or halogenide ions plus halogenidobismuthate(III) groups in $Bi_{12.86}Ni_4X_6$ (*X* = Br, I; Ruck, 1999), results in two-dimensional metals.

Increased oxidation with bromine leads to a mixture of the closely related sub-bromides $Bi_{7-\delta}Ni_2Br_5$ (Wahl *et al.*, 2005) and $Bi_{7-\delta}Ni_2Br_{5-2\delta}$. These pseudo-one-dimensional metals consist of isolated $^1_\infty[Bi_3Ni]$ rods, which are embedded in a salt-like matrix of $[Bi_nBr_{4n+2}]^{(n+2)-}$ groups and bromide ions. Measurements of the electric conductivity on single crystals as well as calculations of the electronic band structure revealed metallic conductivity along [100], whereas in the other directions the compounds are semi-conducting. In low magnetic fields weak but temperature-dependent paramagnetism and, below 9 K, antiferromagnetic ordering were detected. A slight misfit between the metallic and the semi-conducting structure fragments gives rise to modulations. In the previous communication, the crystal structure of $Bi_{7-\delta}Ni_2Br_5$ ($\delta$ = 1/9) was denoted as 'modulation variant 1' associated with the modu-

**Table 1**
Crystallographic data and details of the structure determination of the simplified/average structures of $Bi_{7-\delta}Ni_2Br_{5-2\delta}$ at 293 K.

| | |
|---|---|
| Crystal data | |
| Chemical formula | $Bi_{7-\delta}Ni_2Br_{5-2\delta}$ [$\delta$ = 0.88 (1)] |
| $M_r$ | 1938.8 |
| Crystal system, space group | Orthorhombic, *Cmcm*/*Pmnm* |
| *a*, *b*, *c* (Å) | 4.0660 (4), 23.305 (3), 17.130 (2) |
| *Z* | 4 |
| Radiation type | Mo $K\alpha$ |
| $D_x$ (g cm$^{-3}$) | 7.94 |
| $\mu$ (mm$^{-1}$) | 88.43 |
| Crystal size (mm) | 0.6 × 0.08 × 0.02 |
| Data collection | |
| Diffractometer | Imaging plate diffractometer IPDS-II (Stoe) |
| Absorption correction | Numerical; crystal description optimized using sets of equivalent reflections |
| $T_{max}$, $T_{min}$ | 0.204, 0.02 |
| Measurement limits | $2\theta_{max}$ = 49.08°; $-4 \le h \le 4$, $-26 \le k \le 26$, $-19 \le l \le 19$ |
| No. of measured, independent and observed [$I > 3\sigma(I)$] reflections | 8504/17051, 815/1631, 752/1075 |
| $R_{int}$, $R(\sigma)$ | 0.103/0.114, 0.065/0.078 |
| Refinement | |
| Refinement on | $F^2$ |
| Figures of merit | $R_1$ [752/1074 $I_o > 3\sigma(I_o)$] = 0.039/0.060, $wR_2$(all $I_o$) = 0.078/085 |
| No. of parameters, restrictions | 56/105, none/7 |
| $\Delta\rho_{max}$, $\Delta\rho_{min}$ (e Å$^{-3}$) | +2.92/2.17, −3.05/−2.3 |

lation vector **q** = 8**a***/9. Here we report on 'modulation variant 2' with **q** = **a***/9 + **b***/2, which indeed shows a significant difference in composition, represented by the sum formula $Bi_{7-\delta}Ni_2Br_{5-2\delta}$.

## 2. Experimental

### 2.1. Synthesis

A mixture that contained Bi (chemically pure, Riedel-de Haën; treated with $H_2$ in order to remove oxygen impurities), Ni (99.99%, Aldrich) and $BiBr_3$ (synthesized from the elements at 493 K) in the desired molar ratio was heated in a silica ampoule ($V \simeq 18$ cm$^3$, $p < 1$ Pa) to 793 K. Slow cooling of the melt resulted in the precipitation of black, air-insensitive needles in high yields. X-ray diffraction on powders as well as EDX (energy-dispersive X-ray diffraction) analyses indicated a homogeneous product. Only X-ray diffraction studies on single crystals revealed the presence of two compounds with slightly different diffraction patterns and compositions, $Bi_{7-\delta}Ni_2Br_5$ ($\delta$ = 1/9) and $Bi_{7-\delta}Ni_2Br_{5-2\delta}$ ($\delta$ = 1/9). The coexistence according to the equation

$$Bi_{7-\delta}Ni_2Br_5 \rightleftharpoons Bi_{7-\delta}Ni_2Br_{5-2\delta} + \delta Br_2' \qquad (1)$$

is supported by the observation of epitaxical intergrowth of crystals of the two sub-bromides. As the decomposition pressure of $Bi_{7-\delta}Ni_2Br_{5-2\delta}$ is slightly reduced compared wtih $Bi_{7-\delta}Ni_2Br_5$, the title compound should be favored at higher temperature. Furthermore, an excess of $BiBr_3$ would increase the pressure of the Br-containing gas-phase species and therefore support the formation of the Br-richer $Bi_{7-\delta}Ni_2Br_5$, whereas higher amounts of Ni would have the opposite effect.

### 2.2. Data collection and reduction

An initial investigation of the reciprocal lattice of a single crystal of $Bi_{7-\delta}Ni_2Br_{5-2\delta}$ was performed using a Buerger precession camera with an imaging plate and Zr-filtered Mo radiation. The diffraction images showed an orthorhombic, C-centered main lattice, and in addition weak superstructure reflections and diffuse scattering overlaying the reflections along **a***. Intensity data were collected on an imaging-plate diffraction system IPDS-II (Stoe) using graphite-monochromated Mo $K\alpha$ radiation ($\lambda$ = 0.71073 Å). The raw data were corrected for background, polarization and the Lorentz factor. The microscopic description of the shape of the flat needle was optimized using sets of reflections that are equivalent in the Laue class *mmm* (Stoe & Cie, 1999). Numerical absorption corrections were applied (Stoe & Cie, 2001; Petříček *et al.*, 2000). Finally, all reflections with transmission factors lower than 2% were removed from the data set.

### 2.3. Refinements of the simplified structure and the average structure

The simplified structure was solved with *SHELXL*97 (Sheldrick, 2008) and refined with the *JANA*2000 program package (Petříček *et al.*, 2000; Table 1). As described for $Bi_{7-\delta}Ni_2Br_5$ (Wahl *et al.*, 2005), a simplified structure of $Bi_{7-\delta}Ni_2Br_{5-2\delta}$ can be determined in the space group *Cmcm*, disregarding the observed violation of the reflection conditions for centering. The atoms Bi1, Bi2, Bi3 and Ni define $^1_\infty$[$Bi_3Ni$] rods parallel to [100]. The Br1 are isolated atoms in the structure. The atoms Bi4, Br2, Br3 and Br4 form chains of *trans* edge-sharing [$BiBr_{4/2}Br_{2/2}$] octahedra, which also run parallel to [100]. The latter were refined as split positions, named *A* and *B*, and the displacement parameters of matching sites were set to be equal. The apparent disorder originates from the superposition of two orientations (*A*) and (*B*) of the bromidobismuthate(III) chains that can be mapped on each other by a $4_2$ screw rotation about their central axis. In the course of the refinement, the occupancy of the Br1 site as well as the sum of the occupancies of Bi4*A* and Bi4*B* proved to be significantly lowered. The refined sum formula $Bi_{6.88\ (1)}Ni_2Br_{4.82\ (2)}$, together with the modulation vector and crystal chemical considerations, suggested a coupling of the deficiencies according to $Bi_{7-\delta}Ni_2Br_{5-2\delta}$ and the specialized value of $\delta$ = 1/9. The structure refinement converged to $R1$ = 0.039 [$R_1(752\ I_o > 3\sigma(I_o))$] and $wR_2$ = 0.078 (all data).

Owing to the observation of the main reflections violating the extinction condition of the C-centering, the true average structure has to be described in the space group *Pmnm*. Compared with the simplified structure in *Cmcm*, two crystallographically independent $^1_\infty$[$Bi_3Ni$] rods, [$BiBr_{4/2}Br_{2/2}$] strands and isolated Br ions emerge. Their defining atoms were labeled with an additional suffix 1 or 2. The displacement

**Table 2**
Crystallographic data and details of the structure determination of the superstructure of $Bi_{7-\delta}Ni_2Br_{5-2\delta}$ at 293(1) K.

| | |
|---|---|
| Superspace group | $Pmnm(\alpha\frac{1}{2}0)000$ resp. $Xmnm(\alpha00)000$ |
| Modulation vector | $\mathbf{q} = \mathbf{a}^*/9 + \mathbf{b}^*/2$ resp. $\mathbf{q} = \mathbf{a}^*/9$ |
| No. of measured reflections | 84 857 |
| No. of independent reflections | 7264, 2713 with $I_o > 3\sigma(I_o)$ |
| No. of main reflections | 1629; 1100 with $I_o > 3\sigma(I_o)$ |
| No. of first-order satellites | 2818; 1387 with $I_o > 3\sigma(I_o)$ |
| No. of second-order satellites | 2817; 237 with $I_o > 3\sigma(I_o)$ |
| $R_{int}$, $R(\sigma)$ | 0.151, 0.036 |
| Refinement on | $F^2$ |
| All reflections: $R_1$, $wR_2$ $[I_o > 3\sigma(I_o)]$/ $R_1$, $wR_2$(all $I_o$) | 0.070, 0.087/0.166, 0.090 |
| Main reflections: $R_1$, $wR_2$ $[I_o > 3\sigma(I_o)]$/$R_1$, $wR_2$(all $I_o$) | 0.058, 0.084/0.083, 0.085 |
| First-order satellites: $R_1$, $wR_2$ $[I_o > 3\sigma(I_o)]$/$R_1$, $wR_2$(all $I_o$) | 0.088, 0.111/0.168, 0.119 |
| Second-order satellites: $R_1$, $wR_2$ $[I_o > 3\sigma(I_o)]$/$R_1$, $wR_2$(all $I_o$) | 0.122, 0.185/0.479, 0.324 |
| No. of parameters, restrictions | 213, 7 |
| $\Delta\rho_{max}$, $\Delta\rho_{min}$ (e Å$^{-3}$) | +9.13, −9.18 |

parameters of split positions *A* and *B* were also set to be equal. Only the occupancy number of one Br1 atom, namely Br12, is reduced. The refinement resulted in the figures of merit $R_1$ = 0.067 [$R_1$(1057 $I_o > 3\sigma(I_o)$)] and $wR_2$ = 0.088 (all data). Experimental data for the simplified and average structures are summarized in Table 2.[1]

### 2.4. Refinement of the modulated superstructure

Numerous weak superstructure reflections, which are overlaid by some diffuse scattering along **a***, indicate an (fairly) ordered structure of $Bi_{7-\delta}Ni_2Br_{5-2\delta}$. Owing to the low intensities of these reflections, the superspace approach for modulated structures was applied. The full diffraction pattern (Fig. 1) allows for several indexing possibilities concerning its indexing. A suitable model, fulfilling all chemical conditions (see below), can be obtained by choosing the vector $\mathbf{q} = \mathbf{a}^*/9 + \mathbf{b}^*/2$ in a primitive unit cell which has the same size as the average structure. In agreement with the developed model (see §3.2), the structure can be determined in the superspace group $Pmnm(\alpha\frac{1}{2}0)000$. However, the reflection condition of the *n*-glide plane seems to be violated by five reflections with $I_o > 10\sigma(I_o)$. The superstructure refined in the non-centrosymmetric space group $Pm2m(\alpha\frac{1}{2}0)000$ showed no significant deviations, but strong correlations between the parameters. Therefore, the structure description in the centrosymmetric space group was retained. Owing to technical reasons an alternative setting was used: The modulation vector component **b***/2 was introduced in a superspace centering $(x_1, x_2 + \frac{1}{2}, x_3, x_4 + \frac{1}{2})$ resulting in the superspace group $Xmnm(\alpha00)000$ with $\mathbf{b}' = 2\mathbf{b}$ and $\mathbf{q} = \mathbf{a}^*/9$.

The superstructure could be solved either by the charge-flipping procedure (Palatinus & Chapuis, 2007) or by refinement of a model that was developed based on crystal-chemical considerations. The refinement was carried out using the *JANA*2000 program package. Since the modulation vector showed no significant deviation from the commensurate value of $\mathbf{q} = \mathbf{a}^*/9$, the commensurate option with $t_0 = 0$ was used during the refinement.

On changing the orientation of the concatenated octahedra (*i.e.* applying the $4_2$ screw rotation in the average structure), the *x* coordinate of the atom Bi4 is altered by $\Delta x = 0.5$. An appropriate description for this discontinuous parameter change would require a considerable number of modulation functions. Therefore, the split model from the average and the simplified structures was retained. Similarly, the modulations of the bromine atoms Br2, Br3 and Br4 are better described using the split model. The modulation of the Bi4 atoms was handled by sawtooth functions (Petříček *et al.*, 1995), whereas for the atoms Br2, Br3 and Br4 crenel functions were applied (Petříček *et al.*, 1990). As far as necessary, the occupation modulation of the atoms Br1 was described by a crenel function. The positional modulation of all Br atoms was additionally fitted by one harmonic function.

To simulate the response of the $Bi_3Ni$ strands to the orientation of the octahedra, a Fourier expansion with two harmonic functions for the atoms Bi1 to Bi3 was introduced. Furthermore, fourth-order anharmonic displacement parameters were adopted for these atoms.

Structure refinements verified the developed model. Nevertheless, noise in the data causes some slight deviations. Hence, the width of the modulation crenel and sawtooth functions and their origins were set according to the developed model. To stabilize the refinement, the displacement parameters of the split Br atoms *A* and *B*, and of the Ni atoms

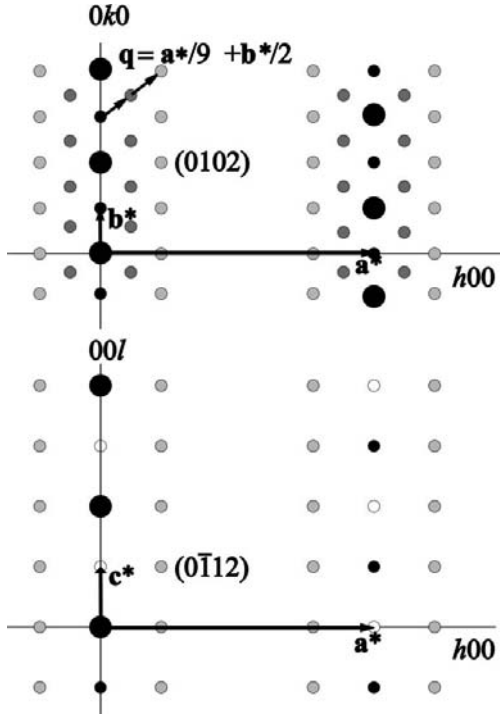


**Figure 1**
Schematic diffraction pattern of the layers *hk*0*m* and *h*0*lm* including the chosen **q** vector. Main reflections are represented in black, first-order satellites in dark gray and second-order satellites in light gray.

[1] Supplementary data for this paper are available from the IUCr electronic archives (Reference: SN5087). Services for accessing these data are described at the back of the journal.

**Table 3**
Selected interatomic distances (Å) in the simplified structure of $Bi_{7-\delta}Ni_2Br_{5-2\delta}$.

| $^1_\infty$[$Bi_3Ni$] rods | | Bromido-bismuthate groups | |
|---|---|---|---|
| Ni—Ni$^{i}$, Ni$^{ii}$ | 2.513 (3) | Bi4*A*—Br4*A*, Br4*A*$^{iii}$ | 2.826 (6) |
| Ni—Bi3 | 2.676 (4) | Bi4*A*—Br2*A*, Br2*A*$^{iv}$ | 2.971 (6) |
| Ni—Bi1, Bi1$^{v}$ | 2.737 (2) | Bi4*A*—Br3*A*, Br3*A*$^{iv}$ | 2.971 (7) |
| Ni—Bi2, Bi2$^{v}$ | 2.775 (2) | | |
| Ni—Bi2$^{i}$ | 2.785 (3) | Bi4*B*—Br4*B*, Br4*B*$^{v}$, Br4*B*$^{vi}$, Br4*B*$^{iii}$ | 2.923 (4) |
| Ni—Bi1$^{i}$ | 2.814 (3) | Bi4*B*—Br3*B* | 2.97 (3) |
| | | Bi4*B*—Br2*B* | 3.02 (3) |
| Bi1—Bi3, Bi3$^{iv}$ | 3.313 (2) | | |
| Bi1—Bi2 | 3.409 (2) | Br1—Bi1$^{v}$, Bi1$^{iii}$ | 3.267 (4) |
| Bi1—Bi2$^{i}$, Bi2$^{vii}$ | 3.597 (2) | Br1—Bi2$^{i}$, Bi2$^{vii}$, Bi2$^{viii}$, Bi2$^{ix}$ | 3.378 (3) |
| | | Br1···Br2*A*, Br2*A*$^{iv}$ | 3.98 (1) |
| Bi2—Bi3, Bi3$^{iv}$ | 3.248 (2) | Br1···Br2*B*, Br2*B*$^{iv}$ | 3.29 (2) |
| Bi2—Bi1 | 3.409 (2) | Br1···Br3*A*$^{x}$ | 3.89 (2) |
| Bi2—Bi1$^{i}$, Bi1$^{vii}$ | 3.597 (2) | Br1···Br3*B*$^{x}$ | 3.08 (3) |
| Bi3—Bi2, Bi2$^{v}$ | 3.248 (2) | | |
| Bi3—Bi1, Bi1$^{v}$ | 3.313 (2) | | |

Symmetry codes: (i) $\frac{1}{2}-x,\frac{1}{2}-y,1-z$; (ii) $-x-\frac{1}{2},\frac{1}{2}-y,1-z$; (iii) $x,y,\frac{1}{2}-z$; (iv) $1+x,y,z$; (v) $x-1,y,z$; (vi) $x-1,y,\frac{1}{2}-z$; (vii) $\frac{3}{2}-x,\frac{1}{2}-y,1-z$; (viii) $\frac{1}{2}-x,\frac{1}{2}-y,z-\frac{1}{2}$; (ix) $\frac{3}{2}-x,\frac{1}{2}-y,z-\frac{1}{2}$; (x) $x+\frac{1}{2},y-\frac{1}{2},z$.

were set to be equal. The introduction of anharmonic displacement parameters of third or higher orders for these atoms resulted in heavy correlations and they were therefore omitted. In total, the refinement involved 213 parameters and converged to $R_1 = 0.070$ [2724 $I_o > 3\sigma(I_o)$] and $wR_2 = 0.090$. Experimental data for the modulated superstructure are summarized in Table 3.

## 3. Results and discussion

### 3.1. The simplified structure and the average structure

The structure of the metal-salt hybrid $Bi_{7-\delta}Ni_2Br_{5-2\delta}$ ($\delta$ = 1/9) can be broken down according to $(Bi_3Ni)_2$-$[Bi_{1-\delta}Br_4]Br_{1-\delta}$ (Fig. 2). The metallic parts, namely $^1_\infty[NiBi_{1/1}Bi_{6/3}]$ rods (Fig. 3), are also known from the intermetallic phase $Bi_3Ni$ (Glagoleva & Zhdanov, 1954; Fjellvåg & Furuseth, 1987; Ruck & Söhnel, 2006), and the subhalides $Bi_{12}Ni_4I_3$ (Ruck, 1997), $Bi_{12.86}Ni_4X_6$ ($X$ = Br, I; Ruck, 1999), and $Bi_{7-\delta}Ni_2Br_5$ ($\delta$ = 1/9; Wahl *et al.*, 2005). The condensation of the capped trigonal antiprisms results in Ni—Ni distances of 2.51 Å, which are close to those of 2.49 Å in Ni metal (Jette & Foote, 1935). The Bi—Ni distances range from 2.68 to 2.81 Å and are almost identical to those in $Bi_3Ni$ (Ruck & Söhnel, 2006). The shortest Bi—Bi distances (3.25–3.60 Å) are in a typical range for (inter)metallic Bi phases (Ruck, 2001*a*,*b*) and slightly longer than in polyhedral $Bi_n^{m+}$ polycations (Kuznetsov *et al.*, 2001). The effective separation of the intermetallic rods by the salt-like anionic part of the structure restricts the metallic conductivity to one dimension (Wahl *et al.*, 2005).

In the simplified structure, the salt-like component $[Bi_{1-\delta}Br_4]Br_{1-2\delta}$ ($\delta$ = 1/9) appears to be heavily disordered. In the chain of *trans* edge-sharing $[BiBr_{2/1}Br_{4/2}]$ octahedra the occupancy of the cation site, Bi4, is reduced to $1-\delta = 8/9$. Furthermore, two different orientations of the $^1_\infty[Bi_{1-\delta}Br_4]$ chains, denoted (*A*) and (*B*), are superimposed. A local $4_2$ screw rotation along their central axes maps them on each other (Fig. 4). The isolated bromine ion, Br1, shows an elongated displacement ellipsoid and its occupancy is reduced to $1-2\delta = 7/9$. Hence, the difference between $Bi_{7-\delta}Ni_2Br_{5-2\delta}$ ($\delta$ = 1/9) and the previously described $Bi_{7-\delta}Ni_2Br_5$ ($\delta$ = 1/9) is essentially a lowered occupancy of the Br1 ion.

### 3.2. Developing a model for the ordered superstructure

The cation vacancies break the $^1_\infty[Bi_{1-\delta}Br_4]$ chain into $[Bi_nBr_{4n+2}]$ oligomers. This corresponds to the empirical finding that owing to short $Bi^{III}$—$Bi^{III}$ distances continuous *trans*-concatenation of $[BiBr_{2/1}Br_{4/2}]$ octahedra is avoided. In all crystal structures with edge-sharing $[BiBr_{2/1}Br_{4/2}]$ octahedra, for example $Bi_6Br_7$ (Benda *et al.*, 1978) or

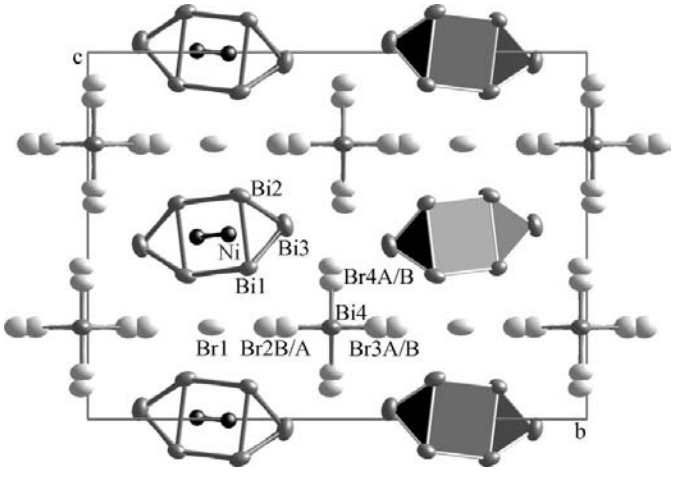


**Figure 2**
Simplified structure of $Bi_{7-\delta}Ni_2Br_{5-2\delta}$ = $(Bi_3Ni)_2[Bi_{1-\delta}Br_{4/2}Br_2]$-$Br_{1-2\delta}$; Bi atoms are dark gray, Br light gray and Ni black. The ellipsoids represent 90% probability at 293 K.

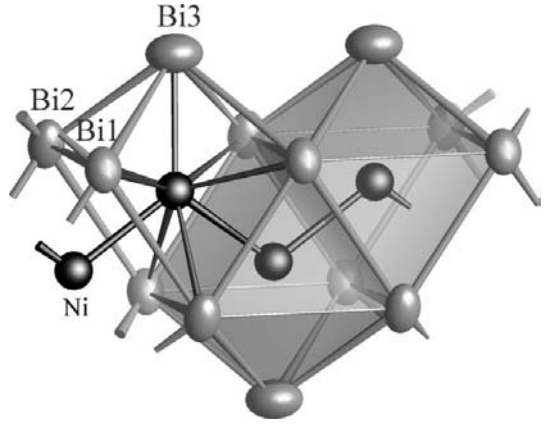


**Figure 3**
Intermetallic rods $^1_\infty[NiBi_{1/1}Bi_{6/3}]$ in the crystal structure of $Bi_{7-\delta}Ni_2Br_{5-2\delta}$.

**Table 4**
Predicted (superstructure model) and refined (simplified and average structure) site occupancies for $Bi_{7-\delta}Ni_2Br_{5-2\delta}$.

| Atom | Predicted occupancy | Refined occupancy: simplified/average structure |
|---|---|---|
| Bi(4*A*) | 9/18 = 0.5 | 0.502 (7)/0.49 (1) |
| Bi(4*B*) | 7/18 = 0.389 | 0.381 (6)/0.39 (1) |
| Br1 | 14/18 = 0.778 | 0.82 (2)/0.80 (2) |
| Br(2*A*) | 11/18 = 0.611 | 0.73 (2)/0.63 (2) |
| Br(3*A*) | 11/18 = 0.611 | 0.73 (2)/0.63 (2) |
| Br(4*A*) | 9/18 = 0.5 | 0.5/0.5 (2) |

$Na_7(BiBr_6)(Bi_2Br_{10})\cdot 18H_2O$ (Lazarini, 1980), the Bi cations are off the polyhedra centers in opposite directions. Of course, this is not an option within a longer series of octahedra.

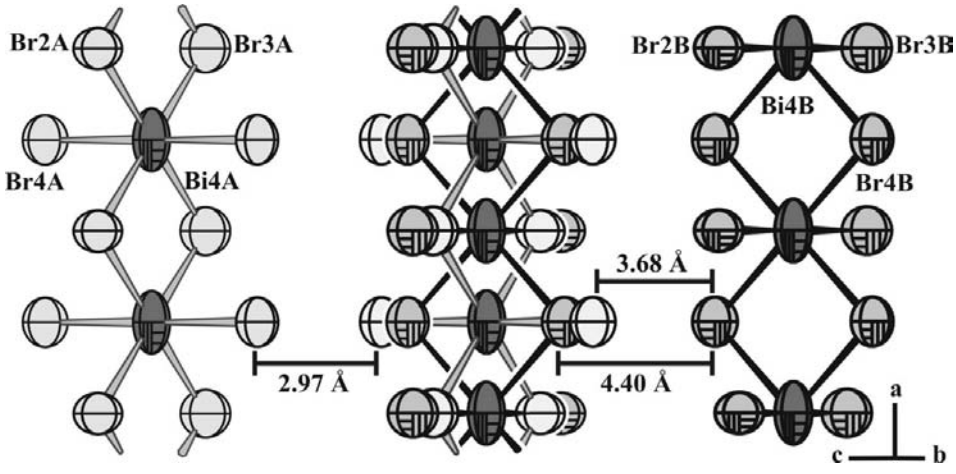


**Figure 4**
Deconvolution of the disorder in the bromido-bismuthate(III) part of the simplified structure (center) into two differently oriented $[BiBr_{2/1}Br_{4/2}]$ chains (left, right), which can be mapped on each other by a local $4_2$ screw rotation along [100].

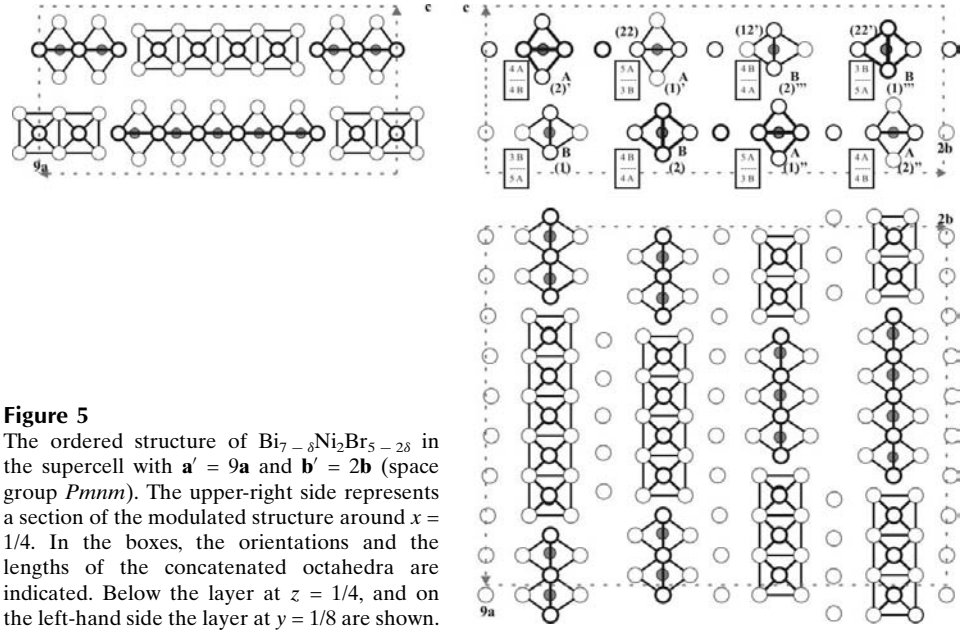

**Figure 5**
The ordered structure of $Bi_{7-\delta}Ni_2Br_{5-2\delta}$ in the supercell with $\mathbf{a}' = 9\mathbf{a}$ and $\mathbf{b}' = 2\mathbf{b}$ (space group *Pmnm*). The upper-right side represents a section of the modulated structure around $x$ = 1/4. In the boxes, the orientations and the lengths of the concatenated octahedra are indicated. Below the layer at $z$ = 1/4, and on the left-hand side the layer at $y$ = 1/8 are shown.

The remaining questions concern length ($n$), orientation ($A$ or $B$) and sequence of the $[Bi_nBr_{4n+2}]$ oligomers. The **q** vector $\mathbf{q} = \mathbf{a}^*/9 + \mathbf{b}^*/2$ allows a commensurate approach with $\mathbf{a}' = 9\mathbf{a}$ and $\mathbf{b}' = 2\mathbf{b}$. Taking the refined occupancies into account, an ordered model of the structure can be developed based on the following considerations:

(i) Ordering along [100]: A cation vacancy in a $^1_\infty[Bi_{1-\delta}Br_4]$ chain with orientation ($A$) would result in an unoccupied octahedron between two $[Bi_nBr_{4n+2}]$ oligomers and thus two isolated Br4*A* atoms. Turning and shifting one oligomer into the ($B$) orientation reduces the void to a tetrahedron and assures that all Br atoms are bonded to Bi atoms. Therefore, any cation vacancy is associated with a change of orientation in the sequence of oligomers along [100].

(ii) Within a period of 9*a*, one vacancy on the Bi4 sites appears and, consequently, only two differently orientated $[Bi_nBr_{4n+2}]$ oligomers. Since *trans*-concatenation is unfavorable, short segments with $3 \le n \le 5$ are to be expected. Sequences like $4(A) + 4(B)$ or $5(A) + 3(B)$ are reasonable. The occupancies, namely 0.5 for Bi4*A* and 0.39 for Bi4*B*, suggest that both sequences appear with the same probability.

(iii) Ordering along [001]: Along this direction, the structure is determined by $[Bi_nBr_{4n+2}]$ oligomers with orientation ($A$). As their terminal Br atoms point along [001], two adjacent strands of the orientation ($A$) would result in unreasonably short Br—Br distances of 2.97 Å (Fig. 4). In accordance with the refined occupancies, alternating orientations are to be expected along [001]. More precisely, a $4(A) + 4(B)$ combination must be enclosed by $5(A) + 3(B)$ sequences (see the right part of Fig. 5).

(iv) Ordering along [010]: Here the $[Bi_nBr_{4n+2}]$ oligomers with orientation ($B$) are crucial. Their terminal Br atoms point onto the isolated Br1 atoms and push them aside, forcing the adjacent strand to adopt orientation ($A$). However, the occurrence of vacancies on the Br1 site opens the alternative that two oligomers of type ($B$) face each other with no Br1 between them. Additionally, two strands of the orientation ($A$) are also possible. A model assuming the sequence

$(A)(A)(B)(B)$ along [010] is in agreement with the doubling of the $b$ axis and the refined occupancies.

Combining conditions (i)–(iv) with the diffraction pattern leads to the model of an ordered structure displayed in Fig. 5. This commensurate approach in the supercell with $\mathbf{a}' = 9\mathbf{a}$ and $\mathbf{b}' = 2\mathbf{b}$ has the symmetry of the centrosymmetric space group *Pmnm*. In fact, the predicted occupation factors match quite well with the refined ones (Table 4) as far as the average structure is concerned. At this point, another important difference between the two closely related structures becomes clear. Here, the ordering results in symmetrically equivalent $[Bi_nBr_{4n+2}]$ oligomers that can be transformed by the center of inversion. In the simplified *Cmcm* structure centers of inversion can be found between the Ni atoms in the $Bi_3Ni$ strands and between neighboring $[Bi_nBr_{4n+2}]$ oligomers in the **c** direction. Hence, the superstructure of $Bi_{7-\delta}Ni_2Br_{5-2\delta}$ can be described in a centrosymmetric space group, namely *Pmnm*, in contrast to $Bi_{7-\delta}Ni_2Br_5$. In the latter structure the equivalent $[Bi_nBr_{4n+2}]$ oligomers are generated *via* the *C*-centering. There the ordering is accompanied by the loss of the center of inversion and the superstructure has to be described in the noncentrosymmetric space group *Cm*2*m*.

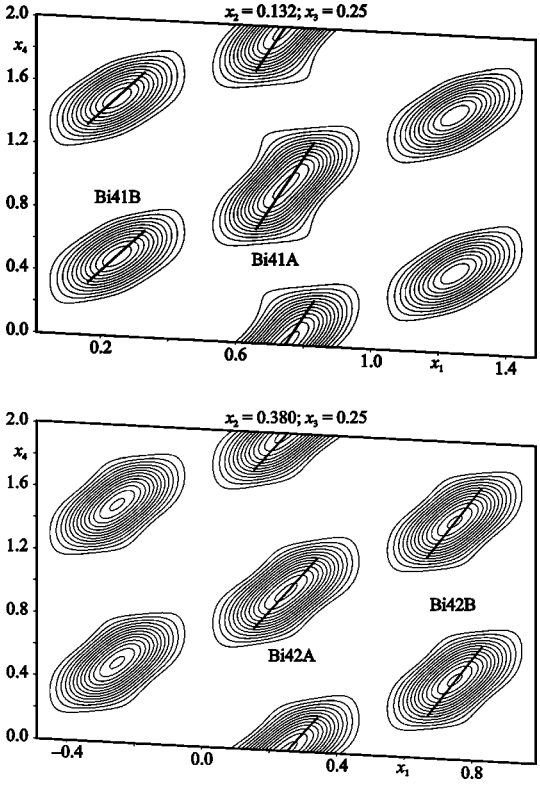


**Figure 6**
The electron-density distributions around the atoms Bi41 and Bi42 in $x_1 - x_4$ constructed from the diffraction pattern including the satellite reflections. The contour lines symbolize steps within 20 e Å$^{-3}$. The bold lines represent the fit of the atomic positions according to the introduced sawtooth functions. In the upper [lower] part of this picture the sequence $5(A) + 3(B)$ $[4(A) + 4(B)]$ is shown.

### 3.3. Verification of the model of the modulated structure of $Bi_{7-\delta}Ni_2Br_{5-2\delta}$

The model of the ordered superstructure with $\mathbf{a}' = 9\mathbf{a}$ and $\mathbf{b}' = 2\mathbf{b}$ in the space group *Pmnm* is equivalent to the description in the [3 + 1]-dimensional superspace group $Pmnm(\alpha\frac{1}{2}0)000$ based on the sub-cell and the commensurate modulation vector $\mathbf{q} = \mathbf{a}^*/9 + \mathbf{b}^*/2$. In general, the Fourier sections ($F_o$) are in good agreement with the developed model.

Fig. 6 shows the modulation of the Bi41 atoms corresponding to the sequence $5(A) + 3(B)$. The two maxima along $x_4$ are well described by the sawtooth function. The position Bi41*B* with $x_1 = 1/4$ is occupied in the interval $3/9 \leq x_4 \leq 6/9$ ($\Delta x_4 = 3/9$) and represents a triplet of octahedra, namely $[Bi_3Br_{14}]$, in orientation $(B)$. It is followed by a $[Bi_5Br_{22}]$ group with orientation $(A)$ in $-5/18 \leq x_4 \leq 5/18$ ($\Delta x_4 = 5/9$), leaving an unoccupied tetrahedron between the chains.

The Fourier plot of the site Bi42 (Fig. 6) shows the sequence $4(A) + 4(B)$. Both Bi atoms represent quadruples of octahedra ($\Delta x_4 = 4/9$), namely $[Bi_4Br_{18}]$, centered at $x_1 = 1/4$, $x_4 = 0$ for Bi42*A*, and at $x_1 = 3/4$, $x_4 = 1/2$ for Bi42*B*. The inclination of the sawtooth function demonstrates that the Bi4 atoms leave the centers of their octahedra. In fact, all distances between the Bi cations in the $[Bi_nBr_{4n+2}]$ oligomers (Bi4—Bi4 distances: 4.28 ± 0.08 Å) are significantly longer than in the simplified structure (4.07 Å).

Fig. 7 displays the modulation along [010]. In the Fourier plot $x_2 - x_4$, with $x_1 = 0.25$ and $x_3 = 0.25$, on the right site of the Br11 atom only the Bi4 atom with $x_1 = 1/4$, namely Bi41*B*, appears for certain $x_4$ (Bi41*A* is in $x_1 = 3/4$). If Bi41*B* is present, then the atoms Br21 and Br31 (with the same $x_4$ coordinate) are in their $(B)$ positions. Otherwise they are found in position $(A)$. The Br11 atom, which is present for all values of $x_4$, is shifted according to the orientation of the strand (1). In the left part of the Fourier plot, the atom Bi42″ occurs for the same $x_4$ as the atom Bi41. Hence, the $[Bi_nBr_{4n+2}]$ oligomers in (1) and (2″) positions are on the

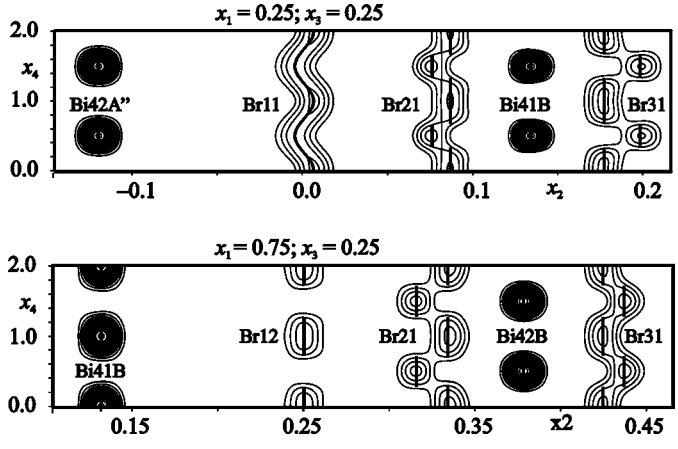


**Figure 7**
The electron-density distributions around the atoms Br11 and Br12 in $x_2 - x_4$. The contour lines symbolize steps within 20 e Å$^{-3}$.

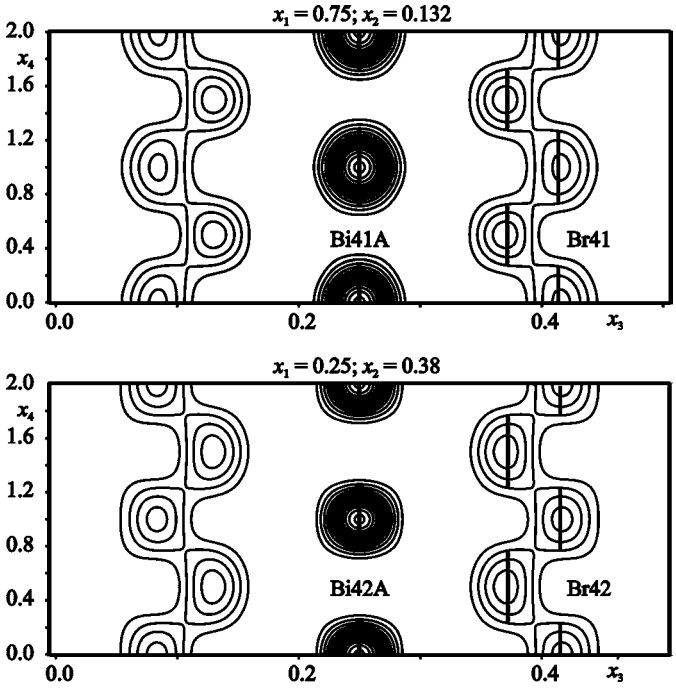


**Figure 8**
The electron-density distributions around the atoms Bi41*A* and Br41 (Bi42*A* and Br42) in $x_3 - x_4$. The contour lines symbolize steps within 20 e Å$^{-3}$.

same level in $x_1$, but strand (2″) must have orientation (*A*), since neither Br22 nor Br32 are visible.

The modulation of the atom Br12 ($x_1 = 0.75$, $x_3 = 0.25$) is notably different (Fig. 7). The atoms Bi41 and Bi42 are present for different $x_4$ coordinates and thus the $[Bi_nBr_{4n+2}]$ oligomers in (1) and (2) positions are shifted relative to each other along $x_1$. The (non-)occurrence of Br atoms in the Fourier plot indicates the same orientation for two neighboring strands. In between two octahedra of orientation (*B*), the position Br12 remains unoccupied, seen as a discontinuous electron density in the Fourier plot. Unphysically short distances as in the simplified structure are not observed. The distance between Br11 and Br32*B* with 3.45 Å is the shortest interhalogen distance in the superstructure.

Along [001] only the Fourier plot of positions (1) and (2) are given (Fig. 8). Again, the modulation of the Br atoms is described well by the adopted functions. The occupation of the positions (*A*) for Bi4 and Br4 are clearly correlated (same $x_4$).

The response of the $^1_\infty[NiBi_{1/1}Bi_{6/3}]$ rods to the different orientations of the bromido-bismuthate(III) groups is rather small. The maximum amplitude of the intermetallic bonds is ±0.13 Å.

The superspace approach should be considered as an approximation to the real crystal structure. The extremely high absorption coefficient of the substance, the poor intensities of the superstructure reflections, the additional diffuse scattering along **a***, which was not included in the structure refinements, as well as the usage of restricted modulation functions do not allow the crystal structure to be determined more precisely. However, the acquired model of the superstructure makes sense from the crystallographic and chemical points of view and the real structure will be very closely related to it.

## 4. Conclusions

The crystal structure of the compound $Bi_{7-\delta}Ni_2Br_{5-2\delta} = [NiBi_{1/1}Bi_{6/3}]_2[Bi_{1-\delta}Br_{4/2}Br_2]Br_{1-2\delta}$ is very similar to the compound $Bi_{7-\delta}Ni_2Br_5$ described earlier. Starting from the disordered simplified structure, an ordered model was obtained by a thorough analysis of occupation factors, the interatomic distances and the diffraction pattern. The usage of the superspace formalism allows an appropriate description of the diffraction data and confirms the 9**a** × 2**b** superstructure.

The authors wish to thank Dr Thomas Doert for helpful discussions and the Deutsche Forschungsgemeinschaft for financial support. We are also indebted to one of the referees for his valuable comments.

## References

Benda, H. von, Simon, A. & Bauhofer, W. (1978). *Z. Anorg. Allg. Chem.* **438**, 53–67.
Fjellvåg, H. & Furuseth, S. (1987). *J. Less-Common Met.* **128**, 177–183.
Giamarchi, T. (2004). *Chem. Rev.* **104**, 5037–5055.
Glagoleva, V. P. & Zhdanov, G. S. (1954). *Zh. Eksp. Teor. Fiz. SSSR*, **26**, 337–344.
Jette, E. R. & Foote, F. (1935). *J. Chem. Phys.* **3**, 606–616.
Kuznetsov, A. N., Kloo, L., Lindsjö, M., Rosdahl, J. & Stoll, H. (2001). *Chem. Eur. J.* **7**, 2821–2828.
Lazarini, F. (1980). *Acta Cryst.* B**36**, 2748–2750.
Palatinus, L. & Chapuis, G. (2007). *J. Appl. Cryst.* **40**, 786–790.
Petříček, V., Dusek, M. & Palatinus, L. (2000). *JANA*2000. Institute of Physics, Praha, Czech Republic.
Petříček, V., Gao, Y., Lee, P. & Coppens, P. (1990). *Phys. Rev. B*, **42**, 387–392.
Petříček, V., van der Lee, A. & Evain, M. (1995). *Acta Cryst.* A**51**, 529–535.
Ruck, M. (1997). *Z. Anorg. Allg. Chem.* **623**, 243–249.
Ruck, M. (1999). *Z. Anorg. Allg. Chem.* **625**, 453–462.
Ruck, M. (2001*a*). *Angew. Chem.* **113**, 1222–1234.
Ruck, M. (2001*b*). *Angew. Chem. Int. Ed.* **40**, 1182–1193.
Ruck, M. & Söhnel, T. (2006). *Z. Naturforsch. B*, **61**, 785–791.
Sheldrick, G. M. (2008). *Acta Cryst.* A**64**, 112–122.
Stoe & Cie (1999). *X-SHAPE* 1.06. Stoe and Cie GmbH, Darmstadt, Germany.
Stoe & Cie (2001). *X-RED*32 1.01. Stoe and Cie GmbH, Darmstadt, Germany.
Wahl, B., Doert, Th., Söhnel, T. & Ruck, M. (2005). *Z. Anorg. Allg. Chem.* **631**, 457–467.